FEBS Letters 586 (2012) 4165–4172

journal homepage: www.FEBSLetters.org

MicroRNA 497 modulates interleukin 1 signalling via the MAPK/ERK pathway

Dongling Zheng, Anna Radziszewska, Patricia Woo *

Division of Infection and Immunity, University College London, 5 University Street, London WC1E 6JF, UK

ARTICLE INFO

Article history:
Received 31 August 2012
Revised 8 October 2012
Accepted 8 October 2012
Available online 22 October 2012

Edited by Tamas Dalmay

Keywords:
ERK pathway
MEK1
IL-1
microRNA
miR-497
IL-6

ABSTRACT

The MAPK/ERK signalling pathway has been described to mediate IL-1 induction of target genes and is known to be regulated by microRNAs (miRNA). We describe a novel miRNA regulating the expression of the MEK1 gene and how it impacts IL-1 induced IL-6 transcription. miR-497 was predicted to target MEK1 3′UTR using bioinformatic tools. Transfection of miR-497 into HeLa cells inhibited MEK1 protein expression by 50%. In transient transfection experiments, the luciferase activity of a MEK1 3′UTR luciferase reporter construct was reduced in the presence of miR-497, and mutation of the predicted miR-497 binding site restored activity. miR-497 also decreased protein levels of RAF1 and ERK1 but not ERK2. Addition of miR-497 was further shown to inhibit IL-1 induced IL-6 gene transcription.

1. Introduction

Interleukin 1 (IL-1) is a key pro-inflammatory cytokine that mediates the expression of multiple genes, thereby contributing to immune and inflammatory responses. Dysregulation of the normal expression patterns of IL-1 and/or its target genes is central in the pathology of autoimmune and auto-inflammatory diseases. Relatively little is known regarding the control of the intracellular signalling pathways once an IL-1 signal is received. IL-1 signals via its Type I receptor through the mitogen-activated protein kinase (MAPK) signalling pathways leading to activation of transcription factors, such as NFκB (nuclear factor κB) and AP-1 (activator protein 1), which then activate multiple genes such as IL-6 and IL-8 [1,2]. There are at least three distinct and parallel MAPK pathways involved: extracellular signal-regulated kinase (ERK), c-Jun amino-terminal kinase (JNK), and p38. The ERK pathway is usually considered as the 'classic' MAPK signalling pathway in which RAF1 (v-raf-1 murine leukaemia viral oncogene homolog 1) mediates phosphorylation of MEK1/2 (MAP kinase kinases 1 and 2), which in turn mediate phosphorylation of ERK1/2 [2]. It is an evolutionarily conserved signal transduction cascade involved in the control of many fundamental cellular processes that lead to cell proliferation, apoptosis, and differentiation.

The control of the expression of these signalling molecules is therefore one of the important steps in transmission of the IL-1 signal within the cell. MicroRNAs (miRNAs) have been observed to regulate the ERK pathway at posttranscriptional level. miRNAs are a class of 19–24 nucleotide long non-coding RNAs that have been regarded as important posttranscriptional regulators of cell differentiation, apoptosis, and proliferation, as well as the immune response [3]. They regulate gene expression by forming imperfect base pairing with sequences in the 3′ untranslated region (3′UTR) of their target mRNAs, leading to mRNA degradation, or inhibition of translation into protein [4]. The 2–8 nucleotides of a miRNA, called the "seed region", are often important for base pairing [5].

It has been shown that miRNA let-7 negatively regulates RAS genes, the upstream signalling molecules of RAF1 in the ERK pathway [6,7]. RAF1 is targeted by miR-497 and miR-125b [8,9]. However, little is known about miRNA control of MEK1 and MEK2 protein expression. In fibroblast cells MEK1 but not MEK2 forms a signalling complex with RAF1 which suggests that in those cells the RAF1 signalling pathway preferentially activates ERKs via MEK1 [10]. We have provided novel evidence in this study that human miR-497 negatively regulates expression of MEK1 in HeLa cells by classic interaction with the MEK1 3′UTR and represses its mRNA translation. We confirmed that miR-497 also targets RAF1 and ERK1, and could impact on inflammatory responses by affecting IL-1β signalling.

Abbreviations: IL, interleukin; MAPK, mitogen-activated protein kinase; NFκB, nuclear factor κB; AP-1, jun proto-oncogene; ERK, extracellular signal-regulated kinase; JNK, c-Jun amino-terminal kinase; P38, mitogen-activated protein kinase 14; MEK, MAP Kinase kinase; RAF1, v-raf-1 murine leukaemia viral oncogene homolog 1; miRNA, microRNA; qPCR, quantitative realtime polymerase chain reaction; 3′UTR, 3′ untranslated region

* Corresponding author. Fax: +44 2076796212.
E-mail address: patricia.woo@ucl.ac.uk (P. Woo).

0014-5793/$36.00
http://dx.doi.org/10.1016/j.febslet.2012.10.014

Table 1
Primer sequences used in this study.

	Forward (5′ → 3′)	Reverse (5′ → 3′)
Cloning		
MEK1-full[a]	CCG*CTCGAG*AAGTGGATTTTGCAGGTTGG	ATTT*GCGGCCGC*TGGTACTTGGATATGGGGAAA
MEK1-short[a]	CCG*CTCGAGT*GCCTGTATTTTCGGGATTC	ATTT*GCGGCCGC*CCAGCTATCATGGCAGTGAA
Mutagenesis		
Mut1[b]	CAGTGCATGTGAAGCATGCTTTGGACGTATGAAA ATGAGCATCAGAGAGT	ACTCTCTGATGCTCATTTTCATACGTCCAAAGCAT GCTTCACATGCACTG
Mut2[b]	CCAGCACACCAACCCATGGACGTGGCGTCTAAGT GTTTGG	CCAAACACTTAGACGCCACGTCCATGGGTTGGTG TGCTGG

[a] Italicised regions indicate the position of restriction enzyme target sequence.
[b] Underlined regions indicate the positions of mutation.

Table 2
MiRNAs predicted to target MEK1 (MAP2K1).

miRNAs	TargetScan			miRANDA scores	PITA scores (<-5)	Target sites		
	Conserved sites		Total Context score			Positions[a]		Alignment
	8mer	7mer-m8						
has-miR-34ac/34bc-5p/449abc/449c-5p								
hsa-miR-34a	**1**	0	-0.38	-0.83	-14.23	Position 573-580	5'	...CUAGCCAGAGCCCUUCACUGCCA...
								:|:|||| |||||||
						hsa-miR-34a	3'	UGUUGGUCGAUUCU-GUGACGGU
hsa-miR-34c-5p	**1**	0	-0.38	-0.83	-12.02	Position 573-580	5'	...CUAGCCAGAGCCCUUCACUGCCA...
								:|: ||| || ||||||
						hsa-miR-34c-5p	3'	CGUUAGUCGAUUGAUGUGACGGA
hsa-miR-449a	**1**	0	-0.38	-0.93	-13.52	Position 573-580	5'	...CUAGCCAGAGCCCUUCACUGCCA...
								|:| | ||||||
						hsa-miR-449a	3'	UGGUCGAUUGUUAUGUGACGGU
hsa-miR-449b	**1**	0	-0.38	-0.93	-13.81	Position 573-580	5'	...CUAGCCAGAGCCCUUCACUGCCA...
								|:| | ||||||
						hsa-miR-449b	3'	CGGUCGAUUGUUAUGUGACGGA
has-miR-15abc/16/16abc/195/322/424/497/1907								
hsa-miR-15a	**1**	0	-0.35	-0.72	-5.98	Position 463-470	5'	...AUGUGAAGCAUGCUUUGCUGCUA...
								:::|| ||| | ||||||
						hsa-miR-15a	3'	GUGUUUGGUAAUACACGACGAU
hsa-miR-15b	**1**	0	-0.35	-0.72	-8.46	Position 463-470	5'	...AUGUGAAGCAUGCUUUGCUGCUA...
								|||:|| |||| ||||||
						hsa-miR-15b	3'	ACAUUUGGUACUACACGACGAU
hsa-miR-16	**1**	0	-0.35	-0.70	-5.82	Position 463-470	5'	...AUGUGAAGCAUGCUUUGCUGCUA...
								:|: || | : ||||||
						hsa-miR-16	3'	GCGGUUAUAAAUGCACGACGAU
hsa-miR-424	**1**	0	-0.35	-0.72	-8.76	Position 463-470	5'	...AUGUGAAGCAUGCUUUGCUGCUA...
								| ::||:|||| |||||||
						hsa-miR-424	3'	AAGUUUUGUACUUAACGACGAC
hsa-miR-497	**1**	0	-0.35	-0.73	-6.26	Position 463-470	5'	...AUGUGAAGCAUGCUUUGCUGCUA...
								:::|| ||:: | ||||||
						hsa-miR-497	3'	UGUUUGGUGUCACACGACGAC
has-miR-96/507/1271								
hsa-miR-96	0	**1**	-0.23	-0.82	-10.37	Position 131-137	5'	...UGAAGAACACAGCAUGUGCCAAG...
								| |:|| || ||||||
						hsa-miR-96	3'	UCGUUUUUACACGAUCACGGUUU
hsa-miR-1271	0	**1**	-0.23	-0.83	-12.31	Position 131-137	5'	...UGAAGAACACAGCAUGUGCCAAG...
								|| | | ||||||
						hsa-miR-1271	3'	ACUCACGAACGAUCCACGGUUC
has-miR-181abcd/4262								
hsa-miR-181a	0	**1**	-0.21	-0.37	-6.21	Position 728-734	5'	...UAAAUGGAAUUAUUUUGAAUGUC...
								|: : |||||||
						hsa-miR-181a	3'	UGAGUGGCUGUCGCAACUUACAA
hsa-miR-181b	0	**1**	-0.21	-0.37	-9.41	Position 728-734	5'	...UAAAUGGAAUUAUUUUGAAUGUC...
								|: : ||||||
						hsa-miR-181b	3'	UGGGUGGCUGUCGUUACUUACAA
hsa-miR-181d	0	**1**	-0.21	-0.37	-8.41	Position 728-734	5'	...UAAAUGGAAUUAUUUUGAAUGUC...
								|: |: ||||||
						hsa-miR-181d	3'	UGGGUGGCUGUUGUUACUUACAA

[a] Positions of seed sequence are relative to the start of the MEK1 3′UTR.

2. Materials and methods

2.1. Prediction of candidate miRNAs binding to MEK1 3′UTR

Three software applications were used to predict potential miRNAs targeting the MEK1 3′UTR: TargetScan 6.1 [11,12], miRANDA [13] and PITA [14]. To maximise our chances of finding real candidates, only those miRNA target sites predicted by all three programs and broadly conserved among vertebrates were considered.

2.2. Cell culture and miRNA transfection

HeLa cells were maintained in DMEM supplemented with 10% FBS in a 37 °C incubator with 5% CO_2.

For miRNA transfection, cells were plated in 24-well plates and incubated for 24 h before transfection. Near confluent cells were transfected with 10 nM of precursor of microRNA (pre-miR, Applied Biosystems) or 10 nM pre-miR in combination with 50 nM miR inhibitor (anti-miR, Applied Biosystems) using Lipofectamine RNAiMAX (Invitrogen) according to the manufacturer's protocol. Cells were collected for RNA and protein analysis at 48 h after transfection.

For IL-1 stimulation, HeLa cells were transfected with miRNAs for 36 h and then incubated in DMEM plus 2% FBS for 12 h, followed by addition of 0.5 ng/ml of IL-1β (Sigma). Cells were collected at 0, 5 min, 15 min, 30 min and 1 h for protein analysis, at 0, 1 h, 3 h, 6 h, 14 h, 24 h for RNA analysis.

2.3. RNA purification and quantitative real-time PCR (qPCR)

Total RNA was extracted using Trizol reagent (Invitrogen) according to the manufacturer's protocol. One microgram of RNA was transcribed into cDNA using Qantitect reverse transcription kit (Qiagen) and qPCR reactions were set up with Taqman gene expression assays (Applied Biosystems) and Solaris qPCR Gene Expression Master Mix (Thermal Scientific). The qPCR reactions were performed on an Eppendorf Mastercycler with cycling conditions as follows: 15 min of denaturation at 95 °C and then 40 cycles of 95 °C for 15 s, 60 °C for 1 min. The RPLP0 gene was used as an endogenous control. Relative levels of mRNA expression of interesting genes were calculated according to the ΔΔCT method [15], normalised by comparison to RPLP0 expression.

2.4. Western blot

Whole cell lysates were resolved by 10% NuPAGE Bis–Tris gel (Invitrogen), transferred to a PVDF membrane (GE Healthcare). The membrane was blocked with 5% bovine serum albumin (Sigma) in tris-buffered saline and 0.1% Tween 20 and then incubated with primary antibodies overnight at 4 °C. The membranes were then incubated with secondary HRP-conjugated antibodies at room temperature and the proteins of interest were visualised with an enhanced chemiluminescence detection system (Thermo Scientific). The membranes were reprobed with antibody against GAPDH to control for any loading differences between lanes. The corresponding bands were quantified by image processing software, ImageJ (NIH, http://rsb.info.nih.gov/ij/). The antibodies for MEK1, p-MEK1, GAPDH, and secondary anti-mouse HRP IgG were obtained from Santa Cruz Biotechnology. The antibodies for ERK1/2, p-Erk1/2, RAF1, P38, p-P38 and anti-rabbit HRP IgG were from Cell Signaling Technology.

2.5. 3′UTR constructs, cotransfection and luciferase reporter assay

The full length and the short fragment of MEK1 3′UTR sequence were amplified from HeLa cDNA using primers incorporating *XhoI* and *NotI* cloning sites. The PCR fragments were then inserted into the 3′ end of the coding sequence of a *Renilla* luciferase gene in the psiCheck-2 vector (Promega). Mutants were generated using a site-directed mutagenesis protocol [16]. The oligonucleotides used in this study are listed in Table 1. All constructs were confirmed by full sequencing.

For cotransfection, HeLa cells were seeded in 96-well plates and cultured for 24 h before transfection with 50 ng of 3′UTR construct or empty vector using Lipofectamine LTX (Invitrogen). Six hours after DNA transfection, cell media were replaced with fresh media and then sequentially transfected with 10 nM of the miRNA precursors. Cell extracts were prepared 48 h after miRNA transfection.

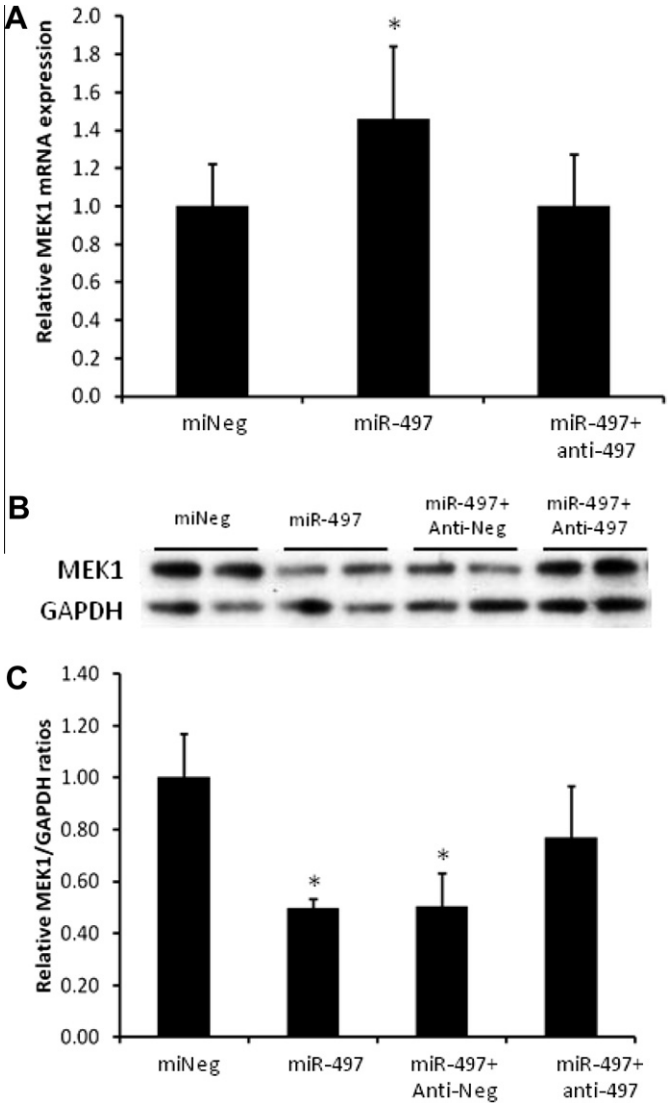

Fig. 1. The effect of miR-497 on MEK1 expression. (A) MEK1 mRNA expression measured by qPCR. HeLa cells were transfected with 10 nM of miRNA precursors alone or in combination of miRNA inhibitor (anti-497) for 48 h and then collected for RNA purification and qPCR analysis. The measurements were normalised to those for the RPLP0 gene before being compared to control. miNeg: miRNA precursor negative control (B) Western blot image of MEK1 protein expression. The image is a representative of three separate experiments. miNeg: miRNA precursor negative control; antiNeg: anti-miR negative control. (C) Quantification of MEK1 protein levels in Western blot analysis. Cell lysates from treated cells described above were subjected to immunoblotting with antibody against MEK1 or GAPDH. The protein bands were quantified by ImageJ (NIH) and normalised to those of GAPDH bands before compared to those measured in miNeg#1-transfected cells (= 1.0). The values are the mean and S.D. from three experiments. $^{*}P < 0.05$ compared to control cells.

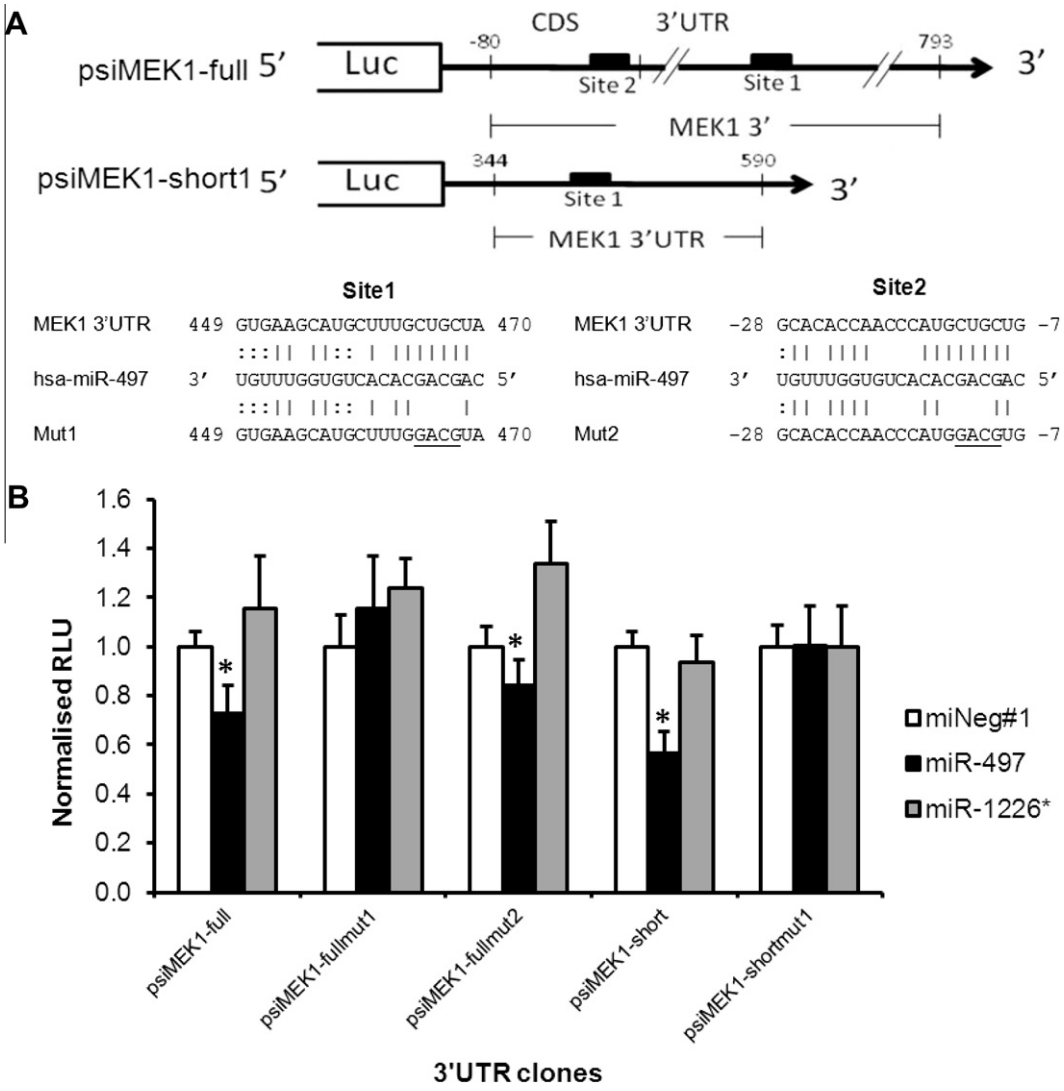

Fig. 2. Validation of miR-497 target sites on MEK1. (A) Schematic structure of MEK1 3′UTR constructs and putative miR-497 binding sites. The basepair positions labelled are relative to the start of MEK1 3′UTR. The sequence to be mutated is underlined. (B) Luciferase activities of the 3′UTR constructs in miRNA transfected HeLa cells. The ratios of *Renilla:Firefly* luciferase activities were first normalised to psiCHECK-2 and expressed as relative to the measurements from miNeg#1 transfected cells. Data shown are the mean and S.D. of three separate experiments. $^{*}P < 0.05$ compared to control cells.

The luciferase activities were measured with a Dual Luciferase Assay System (Promega) and normalised to internal control *Firefly* luciferase activities. The luciferase activity of each construct was compared with that of empty psiCHECK2 vector.

2.6. Statistic analysis

All experiments were repeated at least three times. Data are presented as mean ± S.D. The statistical significance of differences between experimental groups was determined with two-tailed unpaired Student's *t*-test at a significance level of $P < 0.05$.

3. Results

3.1. miR-497 suppresses expression of MEK1 protein

Fourteen potential miRNA binding sites within the MEK1 3′UTR were predicted by TargetScan, miRANDA, and PITA programs and belong to the miR-34, miR-15, miR-96 and miR-181 families (Table 2). Of these candidates, miR-15a, -15b, -16, -424 and -497 share the same 'seed' region and are from the miR-15 superfamily. Many of the family members are associated with altered expression in cancers, neurodegeneration or autoimmune mouse models. We focused on miR-497, the only miRNA within this list that has been reported to be differentially expressed in CD4+ cells in a human autoimmune disease, multiple sclerosis [17].

To evaluate whether miR-497 affects MEK1 expression, HeLa cells were transfected with the miR-497 precursor or the negative control (miNeg#1) for 48 h and MEK1 mRNA and protein levels were measured by qPCR and Western blots respectively. Although, compared to miNeg#1 transfected cells, MEK1 mRNA expression was marginally increased in the miR-497 transfected cells (Fig. 1A), its protein expression was repressed by 50% ($P < 0.05$) (Fig. 1B and C). The effect of miR-497 on MEK1 expression was reversed when miR497 was cotransfected with its specific inhibitor anti-497 (Fig. 1B and C).

3.2. Verification of the miR-497 target sites in the MEK1 3′UTR

Computational analysis revealed a putative binding site (site1) located at 449–470 bp of the MEK1 3′UTR and the PITA program

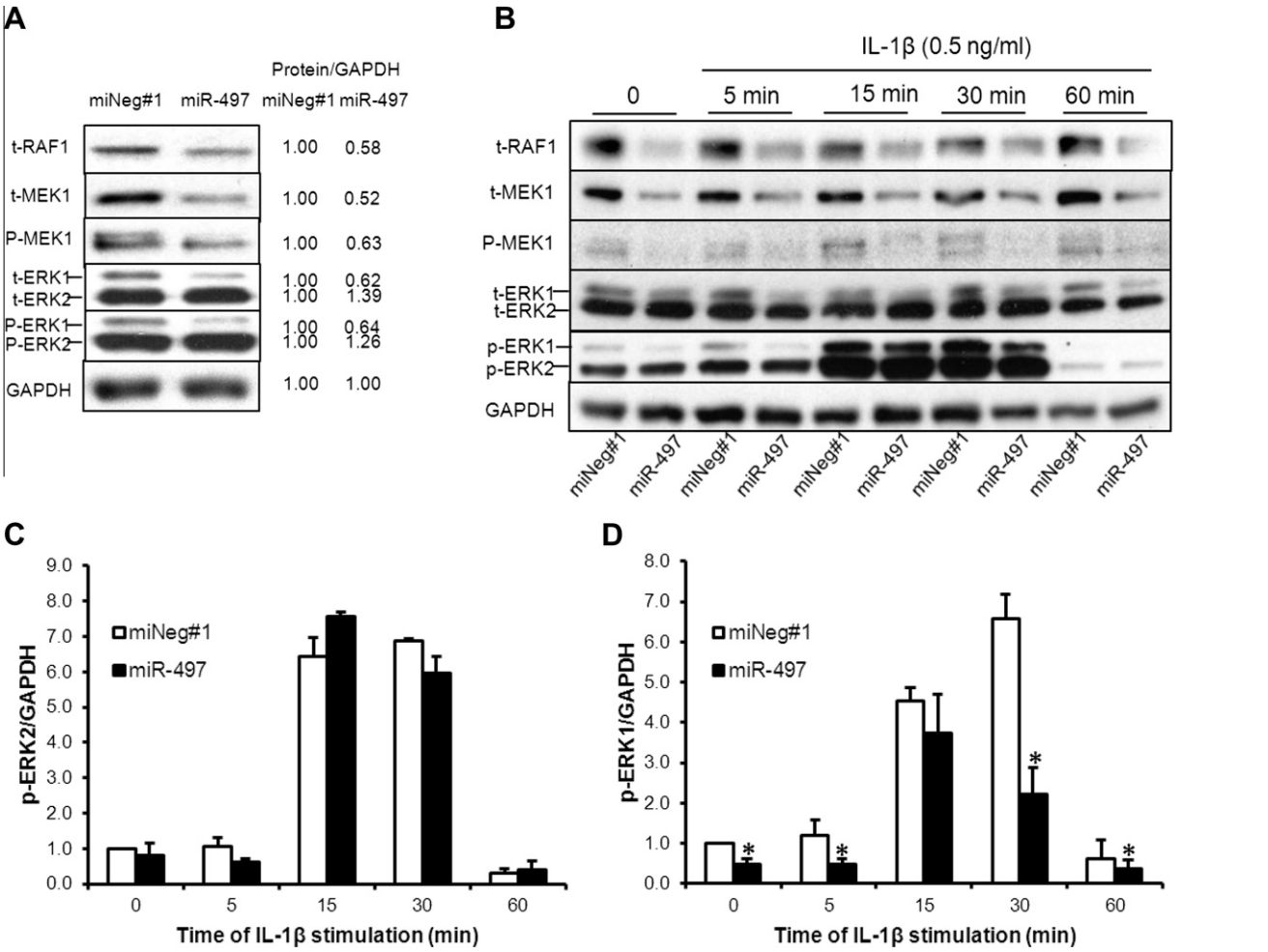

Fig. 3. The effect of miR-497 on the ERK pathway. (A) Western blot images of total (t-) and phosphorylated (p-) protein expression of RAF1, MEK1 and ERK1/2 in miRNA transfected cells described in Fig. 1. The intensities of protein bands were first normalised to those of GAPDH bands and then compared to measurements from miNeg#1-transfected cells. The relative levels are shown on the right. (B) Western blot images of total and phosphorylated protein levels in miRNA transfected cells following IL-1β stimulation. After transfection with miRNAs for 48 h, HeLa cells were treated with 0.5 ng/ml IL-1β. Lysates were collected at 0, 5 min, 15 min, 30 min and 1 h of stimulation and immunoblotted. The images are representatives of three independent experiments. (C) Quantification of p-ERK2 and (D) p-ERK1 of Western blot images. The band intensities were normalised to corresponding GAPDH bands and compared to those at time 0 in control cells. Data shown are the mean and S.D. $^{*}P < 0.05$ compared to corresponding control.

also predicts a second site (site2) located at the end of the coding region (Fig. 2A). To validate these predictions, a luciferase reporter construct containing a full length MEK1 3′UTR at 3′ end of a *Renilla* luciferase gene was generated (psiMEK1-full) and the "seed" region of either site1 or site2 was mutated with a 4 bp substitution (psiMEK1-fullmut1 and psiMEK1-fullmut2, respectively). The wild-type or mutant constructs were cotransfected with the miRNA precursors into HeLa cells.

As shown in Fig. 2B 20% reduction in luciferase activity of the wild-type reporter construct was observed when cotransfected with miR-497 compared to control cells. Furthermore, while overexpression of miR-497 still inhibited luciferase activity of psiMEK1-fullmut2, it had no significant effect on the activity of psiMEK1-fullmut1. Treatment with the miR-1226* precursor, which has no predicted target sites on MEK1 3′UTR, did not affect the luciferase activity of any reporter construct.

To minimise the interference from surrounding sequence, we also generated a reporter construct containing a short 3′UTR fragment covering only site1 (psiMEK1-short). In agreement with results from full-length UTR, luciferase activity of psiMEK1-short was repressed by 40% when cotransfected with miR-497, and the inhibition was completely abolished when site1 was mutated.

3.3. Effect of miR-497 on phosphorylation of MEK1 and other members of the ERK pathway

In the MAPK/ERK cascade, RAF1 mediates phosphorylation of MEK1, which in turn phosphorylates ERK1/2. To elucidate whether the phosphorylation process is affected by miR-497, we measured both total and phosphorylated protein levels of these proteins in miRNA transfected cells. Phosphorylated (p-) MEK1 was reduced to 63% of control levels in miR-497-transfected cells (Fig. 3A) while total protein was reduced to 50% in Fig. 1. Interestingly, ERK1 and ERK2, both of which are normally regulated similarly, showed differential response. Transfection of miR-497 reduced t- and p-ERK1 levels to 62% and 64%, respectively, of expression in control cells while neither ERK2 forms were significantly changed. Consistent with published literature, t-RAF1 level was significantly inhibited by miR-497 [18].

We next treated the miRNA transfected cells with 0.5 ng/ml of IL-1β to examine their response to stimulus. As shown in Fig. 3B, in cells transfected with either miR-497 or the control miNeg#1, IL-1β had no effect on total protein levels of RAF1, MEK1 and ERK1/2. Phosphorylation of MEK1 and ERK1/2 were induced by IL-1β, reaching peak between 15 and 30 min after stimulation

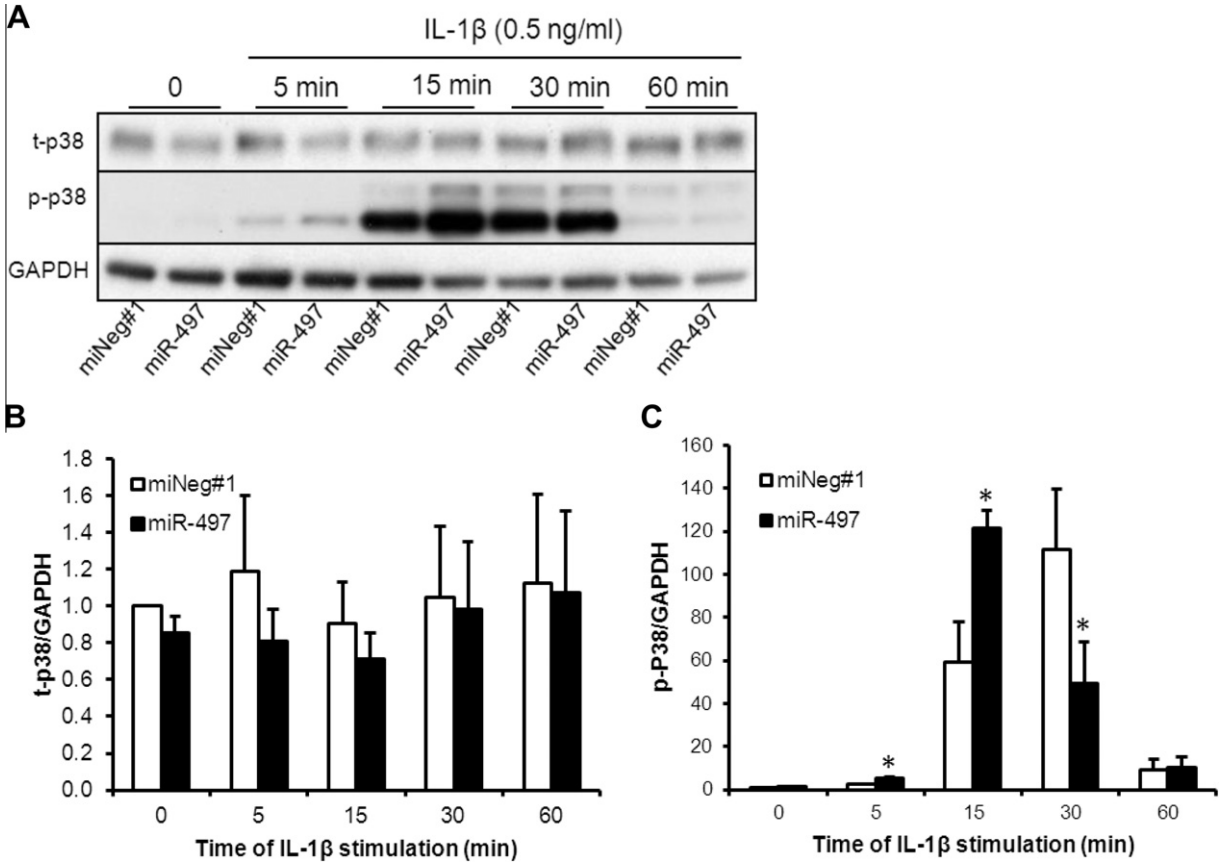

Fig. 4. The effect of miR-497 on p38 activation. (A) Western blot images of total and phosphorylated p38 from IL-1β stimulation experiments measured at different time points after addition of IL-1. (B) Quantification of Western blot images of total protein t-p38/GAPDH from three separate experiments. (C) Quantification of Western blot images of phospho-p38 from three experiments. $^{*}P < 0.05$, comparison between cells transfected with miR-497 and its corresponding control transfected cells.

and declining to below baseline at 1 h in all the replicates. However, miR-497 transfected cells had notably less p-MEK1 and p-ERK1 than control cells at all time points following IL-1β stimulation while p-ERK2 did not seem to change (Fig. 3B and C). Further quantitation indicated that not only were the maximum p-ERK1 levels lower in cells with miR-497 than in control cells, but also dephosphorylation appeared to occur earlier, showing decline at 30 min (Fig. 3D).

3.4. Effect of miR-497 on p38 pathway

To see if there were also changes in the p38 pathway upon IL-1β stimulation in miRNA transfected cells, we checked the levels of t-p38 and p-p38 by Western blot. Total p38 levels were not significantly affected by introduction of miR-497 to HeLa cells before and after IL-1beta stimulation (Fig. 4A and B), implying that p38 is not a direct target of miR-497. By contrast, phosphorylation of p38 displayed a different response pattern between cells transfected with miR-497 and miNeg#1 (Fig. 4A and C). Relatively higher levels of p-p38 were detected in miR-497-transfected cells at 5 and 15 min after stimulation, nearly twice the levels in corresponding control cells. However, dephosphorylation of p38 already occurred after 30 min of stimulation in miR-497 transfected cells while its phosphorylation continued to be high in control cells. This early dephosphorylation in miR-497 transfected cells mirrors what occurred in the phosphorylation of ERK1 (Fig. 3D). At the end of 48 h of stimulation, p-p38 from both cells returned to similar low levels.

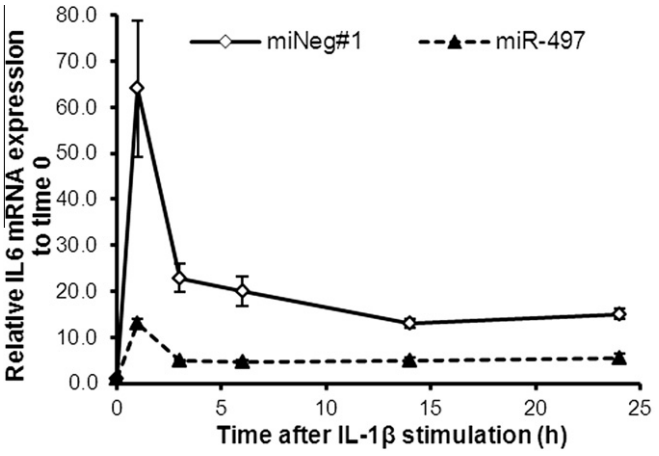

Fig. 5. Expression of IL-6 mRNA in miRNA-transfected cells following IL-1β stimulation. Cells were transfected with miRNAs for 48 h, followed by the addition of 0.5 ng/ml IL-1β and collected at different time points afterwards for qPCR analysis. The data presented are mean and S.D. of fold changes from the basal level at time 0.

3.5. miR-497 affects IL-1-stimulated IL-6 gene transcription

Since IL-1β stimulates production of other cytokines, typically IL-6, via p38 and ERK pathways in HeLa cells [19], it was relevant to examine if miR-497 may influence IL-6 expression. As shown in Fig. 5, IL-1 induction of IL-6 was significantly repressed by

introduction of miR-497. Upon IL-1β stimulation, IL-6 mRNA level was induced by 65-fold at 1 h in the control cells, dropped dramatically to 23-fold at 3 h and then gradually decreased to less than 14-fold after 14 h until the end of the experiment at 24 h. By contrast, in the miR-497-transfected cells, IL-6 expression was induced by only 13-fold and then decreased to and stayed at 5-fold after 3 h.

4. Discussion

Many target prediction tools for miRNAs have been developed based on a combination of stringency of miRNA:mRNA seed pairing, site location, conservation, accessibility, and presence of multiple sites. The sets of predicted target genes from different tools do not overlap well [20]. We have applied three most frequently used programs to predict miRNA regulators of the MEK1 gene. TargetScan considers seed pairing, target site location and conservation; miRANDA weighs seed pairing as well as paring elsewhere and also estimates site accessibility; PITA also considers the seed pairing but estimates the free energy cost to unfold the miRNA:RNA structure. The combination of multiple programs can be useful to narrow down candidates and increase the chance to find true regulators as demonstrated by this study.

We have shown experimentally that miR-497 is a negative regulator of MEK1 protein expression through directly binding to the 3′UTR of the mRNA. Posttranscriptional regulation of MEK1 by miRNA is not unique to miR-497. Recent studies showed that both miR-1826 and miR-424 were negatively correlated with MEK1 protein levels [21,22].

Therefore MEK1 is subject to regulation by multiple miRNAs, which may contribute to tissue or disease-specific modulation of MEK1 activity.

Our results demonstrate for the first time that miR-497 simultaneously inhibits protein levels of three members of the ERK pathway, RAF1, MEK1 and ERK1. miR-497 along with miR-195 (also a member of miR-15 family) have been shown by others to negatively regulate RAF1 protein expression in breast cancer [9]. Lower p-MEK1 seen in this study is likely to be a combined effect of lowered MEK1 and RAF1 protein levels induced by miR497. Lower expression of p-ERK1/2 was also observed in this report but it was regarded as the result of impairment of RAF1 activation. Our results suggest that ERK1 may also be a target of miR-497 in HeLa cells, consistent with an earlier study showing that miR-15 family members targeted ERK1 3′UTR in Neuro2a cells [23]. Since ERK2 phosphorylation has not been affected in our studies, the differential phosphorylation of ERK 1 and 2 observed is less likely to be the upstream effect of miR-497 on RAF 1.The reduction of ERK1 phosphoproteins is more likely to be due to loss of total proteins. However, upon stimulation by IL-1β, we found not only lower induction of ERK1 phosphorylation but also earlier dephosphorylation, thus indicating that a more complex mechanism is involved.

Suppression with ERK or p38 pathway inhibitors reduces IL-1 or TNF stimulated IL-6 expression [19,24], and this phenomenon is also seen in our experiments where the actual fold increase of IL-6 mRNA on IL-1 stimulation was reduced in the presence of transfected miR497. Crosstalk between the ERK and p38 pathways has been described [25,26], where inhibition of MEK1 activity by MEK1 inhibitor, PD98059, resulted in an increase of p38 activity, and vice versa. This may explain the higher p38 phosphorylation levels following IL-1 stimulation in miR-497-transfected cells in our study. It is evident that multiple levels of control of IL-1 intracellular signalling by miRNAs already described [27–29] will need further characterisation.

In the context of autoimmune diseases, an abnormal ERK pathway in T lymphocytes is understood to play a part in initiation and progression of disease [30,31]. As a regulator of the ERK pathway, miR-497 and other members of miR-15 family may play important roles in the immune dysregulation observed in these diseases. For example, miR-497 has been shown to be differentially expressed in CD4 cells, CD8 cells and B cells in relapsing-remitting multiple sclerosis (MS) patients compared to healthy volunteers [17].

In summary, we have shown for the first time that miR-497 is one of the regulators of MEK1, in addition to RAF1, and plays a part in modulating the inflammatory signal of IL-1 to one of its target genes. Elucidating the role of microRNAs in regulating inflammatory pathways may present us with an exciting new avenue in autoimmune disease research.

Acknowledgements

The authors appreciate Dr. Dimitrios Lagos (UCL) for advice on cotransfection and Professor Steve Humphries for comments on the manuscript. This research was supported by the Arthritis Research UK (No. 17287).

References

[1] O'Neill, L.A.J. and Dinarello, C.A. (2000) The IL-I receptor/toll-like receptor superfamily: crucial receptors for inflammation and host defense. Immunol. Today 21, 206–209.
[2] Cobb, M.H. and Goldsmith, E.J. (1995) How MAP kinases are regulated. J. Biol. Chem. 270, 14843–14846.
[3] He, L. and Hannon, G.J. (2004) MicroRNAs: small RNAs with a big role in gene regulation. Nat. Rev. Genet. 5, 522–531.
[4] Bartel, D.P. (2009) MicroRNAs: target recognition and regulatory functions. Cell 136, 215–233.
[5] Miranda, K.C., Huynh, T., Tay, Y., Ang, Y.-S., Tam, W.-L., Thomson, A.M., Lim, B. and Rigoutsos, I. (2006) A pattern-based method for the identification of microRNA binding sites and their corresponding heteroduplexes. Cell 126, 1203–1217.
[6] Kumar, M.S., Erkeland, S.J., Pester, R.E., Chen, C.Y., Ebert, M.S., Sharp, P.A. and Jacks, T. (2008) Suppression of non-small cell lung tumor development by the let-7 microRNA family. Proc. Natl. Acad. Sci. USA 105, 3903–3908.
[7] Oh, J.S., Kim, J.J., Byun, J.Y. and Kim, I.A. (2010) Lin28-let7 modulates radiosensitivity of human cancer cells with activation of K-Ras. Int. J. Radiat. Oncol. Biol. Phys. 76, 5–8.
[8] Hofmann, M.H., Heinrich, J., Radziwil, G. and Moelling, K. (2009) A short hairpin DNA analogous to miR-125b inhibits C-Raf expression, proliferation, and survival of breast cancer cells. Mol. Cancer Res. 7, 1635–1644.
[9] Li, D. et al. (2011) Analysis of MiR-195 and MiR-497 expression, regulation and role in breast cancer. Clin. Cancer Res. 17, 1722–1730.
[10] Jelinek, T., Catling, A.D., Reuter, C.W.M., Moodie, S.A., Wolfman, A. and Weber, M.J. (1994) RAS and RAF-1 form a signalling complex with MEK-1 but not MEK-2. Mol. Cell. Biol. 14, 8212–8218.
[11] Friedman, R.C., Farh, K.K.H., Burge, C.B. and Bartel, D.P. (2009) Most mammalian mRNAs are conserved targets of microRNAs. Genome Res. 19, 92–105.
[12] Lewis, B.P., Burge, C.B. and Bartel, D.P. (2005) Conserved seed pairing, often flanked by adenosines, indicates that thousands of human genes are microRNA targets. Cell 120, 15–20.
[13] Betel, D., Koppal, A., Agius, P., Sander, C. and Leslie, C. (2010) Comprehensive modeling of microRNA targets predicts functional non-conserved and non-canonical sites. Genome Biol., 11.
[14] Kertesz, M., Iovino, N., Unnerstall, U., Gaul, U. and Segal, E. (2007) The role of site accessibility in microRNA target recognition. Nat. Genet. 39, 1278–1284.
[15] Pfaffl, M.W. (2001) A new mathematical model for relative quantification in realtime RT-PCR. Nucl. Acids Res., 29.
[16] Scott, S.P., Teh, A., Peng, C. and Lavin, M.F. (2002) One-step site-directed mutagenesis of ATM cDNA in large (20 kb) plasmid constructs. Hum. Mutat. 20, 323.
[17] Lindberg, R.L., Hoffmann, F., Mehling, M., Kuhle, J. and Kappos, L. (2010) Altered expression of miR-17-5p in CD4+ lymphocytes of relapsing-remitting multiple sclerosis patients. Eur. J. Immunol. 40, 888–898.
[18] Li, D. et al. (2011) Analysis of MiR-195 and MiR-497 expression, regulation and role in breast cancer. Clin. Cancer Res. 17, 1722–1730.
[19] Yang, H.T., Cohen, P. and Rousseau, S. (2008) IL-1 beta-stimulated activation of ERK1/2 and p38 alpha MAPK mediates the transcriptional up-regulation of IL-6, IL-8 and GRO-alpha in HeLa cells. Cell. Signal. 20, 375–380.
[20] Saito, T. and Saetrom, P. (2010) MicroRNAs – targeting and target prediction. N. Biotechnol. 27, 243–249.
[21] Nakashima, T. et al. (2010) Down-regulation of mir-424 contributes to the abnormal angiogenesis via MEK1 and cyclin E1 in senile hemangioma: its implications to therapy. PLoS One 5.

[22] Hirata, H., Hinoda, Y., Ueno, K., Nakajima, K., Ishii, N. and Dahiya, R. (2012) MicroRNA-1826 directly targets beta-catenin (CTNNB1) and MEK1 (MAP2K1) in VHL-inactivated renal cancer. Carcinogenesis 33, 501–508.
[23] Hebert, S.S. et al. (2010) Genetic ablation of Dicer in adult forebrain neurons results in abnormal tau hyperphosphorylation and neurodegeneration. Hum. Mol. Genet. 19, 3959–3969.
[24] Leonard, M., Ryan, M.P., Watson, A.J., Schramek, H. and Healy, E. (1999) Role of MAP kinase pathways in mediating IL-6 production in human primary mesangial and proximal tubular cells. Kidney Int. 56, 1366–1377.
[25] Shimo, T., Matsumura, S., Ibaragi, S., Isowa, S., Kishimoto, K., Mese, H., Nishiyama, A. and Sasaki, A. (2007) Specific inhibitor of MEK-mediated cross-talk between ERK and p38 MAPK during differentiation of human osteosarcoma cells. J. Cell Commun. Signal. 1, 103–111.
[26] Xiao, Y.Q., Malcolm, K., Worthen, G.S., Gardai, S., Schiemann, W.P., Fadok, V.A., Bratton, D.L. and Henson, P.M. (2002) Cross-talk between ERK and p38 MAPK mediates selective suppression of pro-inflammatory cytokines by transforming growth factor-beta. J. Biol. Chem. 277, 14884–14893.
[27] Bhaumik, D., Scott, G.K., Schokrpur, S., Patil, C.K., Orjalo, A.V., Rodier, F., Lithgow, G.J. and Campisi, J. (2009) MicroRNAs miR-146a/b negatively modulate the senescence associated inflammatory mediators IL-6 and IL-8. Aging 1, 402–411.
[28] Ceppi, M., Pereira, P.M., Dunand-Sauthier, I., Barras, E., Reith, W., Santos, M.A. and Pierre, P. (2009) MicroRNA-155 modulates the interleukin-1 signaling pathway in activated human monocyte-derived dendritic cells. Proc. Natl. Acad. Sci. USA 106, 2735–2740.
[29] Tang, B. et al. (2010) Identification of MyD88 as a novel target of miR-155, involved in negative regulation of *Helicobacter pylori*-induced inflammation. FEBS Lett. 584, 1481–1486.
[30] Deng, C., Kaplan, M.J., Yang, J., Ray, D., Zhang, Z.Y., McCune, W.J., Hanash, S.M. and Richardson, B.C. (2001) Decreased Ras-mitogen-activated protein kinase signaling may cause DNA hypomethylation in T lymphocytes from lupus patients. Arthritis Rheum. 44, 397–407.
[31] Ohori, M. (2008) ERK inhibitors as a potential new therapy for rheumatoid arthritis. Drug News Perspect. 21, 245–250.